THE JOURNAL OF BIOLOGICAL CHEMISTRY VOL. 287, NO. 40, pp. 33480–33487, September 28, 2012
Published in the U.S.A.

Regulator of G-Protein Signaling 3 Isoform 1 (PDZ-RGS3) Enhances Canonical Wnt Signaling and Promotes Epithelial Mesenchymal Transition*[S]

Received for publication, March 13, 2012, and in revised form, August 1, 2012 Published, JBC Papers in Press, August 2, 2012, DOI 10.1074/jbc.M112.361873

Chong-Shan Shi, Ning-Na Huang, and John H. Kehrl[1]

From the B-Cell Molecular Immunology Section, Laboratory of Immunoregulation, NIAID, National Institutes of Health, Bethesda, Maryland 20892

Background: Wnt signaling is subject to regulation by regulator of G-protein signaling domain-containing proteins.
Results: PDZ-RGS3 binds GSK3β and inhibits its activity.
Conclusion: PDZ-RGS3 enhances canonical Wnt signaling.
Significance: PDZ-RGS3 expression may promote epithelial to mesenchymal transition.

The Wnt β-catenin pathway controls numerous cellular processes including cell differentiation and cell-fate decisions. Wnt ligands engage Frizzled receptors and the low-density-lipoprotein-related protein 5/6 (LRP5/6) receptor complex leading to the recruitment of Dishevelled (Dvl) and Axin1 to the plasma membrane. Axin1 has a regulator of G-protein signaling (RGS) domain that binds adenomatous polyposis coli and Gα subunits, thereby providing a mechanism by which Gα subunits can affect β-catenin levels. Here we show that Wnt signaling enhances the expression of another RGS domain-containing protein, PDZ-RGS3. Reducing PDZ-RGS3 levels impaired Wnt3a-induced activation of the canonical pathway. PDZ-RGS3 bound GSK3β and decreased its catalytic activity toward β-catenin. PDZ-RGS3 overexpression enhanced Snail1 and led to morphological and biochemical changes reminiscent of epithelial mesenchymal transition (EMT). These results indicate that PDZ-RGS3 can enhance signals generated by the Wnt canonical pathway and that plays a pivotal role in EMT.

Wnt signaling regulates many cellular functions including cell proliferation, differentiation, survival, polarity, and migration (1–3). In the absence of a Wnt signal, cytosolic β-catenin associates with and is phosphorylated by a destruction complex whose core components are Axin1, adenomatous polyposis coli, and two kinases: casein kinase 1 and glycogen synthase kinase 3 α/β (GSK3α/β). The phosphorylated β-catenin is ubiquitinated and is delivered to the proteasome for degradation. As a consequence, cytosolic β-catenin levels remain low and Wnt target genes repressed. The binding of Wnts to Frizzled receptors and LRP5/6 receptor complex induces low-density-lipoprotein-related protein (LRP)[2] phosphorylation and recruitment of the destruction complex. Phosphorylated β-catenin is no longer ubiquitinated and destroyed, and cytosolic β-catenin levels rise (4). This results in its nuclear translocation where it facilitates T cell-specific transcription factor (TCF)-mediated gene expression (5). Canonical Wnt signaling causes the stabilization of Snail1, which represses E-cadherin expression and induces epithelial cells to adopt a mesenchymal morphology, *i.e.* epithelial-mesenchymal transition (EMT) (6–8). This occurs during embryonic morphogenesis and is exploited by metastatic tumors (9, 10). Recently, EMT has been closely associated with both invasive and stem cell properties of cancer cells (11).

Axin1 has a regulator of G-protein signaling (RGS) domain, which has been linked to both G_o- and G_s-mediated stabilization of β-catenin (12). Whereas the Axin1 RGS domain binds adenomatous polyposis coli, it can also bind $G\alpha_s$ in its transition state, activated $G\alpha_{12}$ (*i.e.* GTP-bound), and $G\alpha_o$, irrespective of its GDP- or GTP-binding status. The Axin1 RGS domain differs from the canonical RGS domain in that it lacks key amino acids needed to enhance the GTPase activity of Gα subunits (13). Most members of the RGS protein family possess an RGS domain that binds $G\alpha_i$ and $G\alpha_q$ family members when they are in the transition state, significantly enhancing their intrinsic GTPase activity. The majority of the RGS proteins do not bind $G\alpha_s$ or $G\alpha_{12}$ family members irrespective of their GTP/GDP-binding state. Whereas some RGS proteins consist largely of their RGS domain, other RGS proteins like Axin1 possess additional domains, which can target other proteins and extend their function beyond that assigned to the RGS domain (14, 15). PDZ-RGS3 is a widely expressed isoform of RGS3, which contains several additional domains. At its N terminus is a PDZ domain, which can bind type B ephrins via their C-terminal PDZ-binding motif. It also has an ATP/GTP-binding site and a proline-rich region of unknown function (16, 17). It is known to regulate ephrin-B reverse signaling and chemoattraction (17). It also has been implicated in maintaining the

* This work was supported, in whole or in part, by the intramural research program of the NIAID, National Institutes of Health.
[S] This article contains supplemental Figs. S1 and S2.
[1] To whom correspondence should be addressed: B-Cell Molecular Immunology Section, Laboratory of Immunoregulation, NIAID, National Institutes of Health, 10 Center Dr., MSC 1876, Bethesda, MD 20892. Tel.: 301-443-6907; E-mail: jkehrl@niaid.nih.gov.
[2] The abbreviations used are: LRP, low-density-lipoprotein-related protein; TCF, T cell-specific transcription factor; RGS, regulator of G-protein signaling; Dvl, Dishevelled; EMT, epithelial mesenchymal transition; MDCK, Madin-Darby canine kidney; FRAT, frequently rearranged in advanced T cell.

balance between self-renewal and differentiation of neural progenitor cells (18).

Here, we provide evidence that Wnt β-catenin signal enhances PDZ-RGS3 expression. PDZ-RGS3 helps stabilize β-catenin resulting in increased expression of genes controlled by β-catenin-TCF. Overexpression of PDZ-RGS3 stabilizes Snail1 and can trigger EMT.

EXPERIMENTAL PROCEDURES

Cell Lines and Antibodies—HEK 293 and Madin-Darby canine kidney (MDCK) cell lines were obtained from the American Tissue Culture Collection (Manassas, VA). The cells were maintained in DMEM with 10% fetal bovine serum. The antibodies against the following proteins were purchased: c-Myc, Dvl, Snail1, and actin (Santa Cruz Biotechnology, Santa Cruz, CA); Au1 and Myc (Covance, Princeton, NJ); β-catenin and fibronectin (Sigma-Aldrich); E-cadherin and Ser-33/Ser-37/Thr-41 β-catenin (Cell Signaling Technology, Danvers, MA); cyclin D1 and GSK3β (BD Biosciences, San Jose, CA), RGS3 (Torrey Pines Biolabs, Secaucus, NJ).

Generation of Stable Cell Line and shRNAs—The coding regions of human PDZ-RGS3 and RGS3 were fused to GFP using pEGFP-N1 vector (Clontech Laboratories). The resulting constructs along with the parental construct were transfected into MDCK cells using Lipofectamine 2000 (Invitrogen) following the manufacturer's directions. The day following transfection, the cells were placed under selection with G418 (500 μg/ml) for 4 weeks. The GFP-positive cells were sorted once by flow cytometry to select for high expressing cells. The sequences used for the PDZ-RGS3 shRNAs were as follows: shRNA1, 5′-TGAGAGGCCTGTGGAGCAC and shRNA2, 5′-GACAGTGCAGACCATGAAG. The sequence of the control shRNA that targeted GFP was shRNA, 5′-GCAGAAGAACGGCATCAAG. They were cloned into pSIREN-RetroQ vector (Clontech Laboratories).

Immunoprecipitations—Whole cell lysates for immunoblotting and immunoprecipitations were prepared as follows. 2×10^6 cells were lysed with 0.5 ml of the following buffer (20 mM HEPES, pH 7.4, 2 mM EGTA, 50 mM β-glycerophosphate, 1% Triton X-100, 10% glycerol, and 2 mM Na_3VO_4) along with a protease inhibitor mixture. In some instances 0.5% CHAPS was added. To immunoprecipitate specific proteins, the cells lysates were incubated with 1 or 2 μg of the appropriate antibody for 2 h at 4 °C, and the immunoprecipitates were collected with protein-G-conjugated-Sepharose 6B beads (Santa Cruz Biotechnology) for 1 h at 4 °C. The beads were washed 8 times using 0.5 ml of the above buffer prior to the addition of SDS sample buffer. The samples were fractionated by SDS-PAGE and transferred to nitrocellulose membrane for immunoblotting. To detect cytosolic β-catenin levels by immunoblotting, the cells were lysed in the following buffer: 10 mM Tris-HCl, pH 7.4, 10 mM NaCl, 3 mM $MgCl_2$, and 0.25% Nonidet P-40. After 10 min on ice, the lysates were centrifuged for 5 min at 1,500 rpm. Membranous and cytosolic materials were obtained by ultracentrifugation at 30,000 rpm (100,000 × *g*) for 90 min at 4 °C. The supernatant was designated as the cytosolic fraction, and pellets were designated the membranous fraction. β-Catenin was analyzed by separation of 30 μg of cytosolic proteins on SDS-10%-polyacrylamide gels and immunoblotting with an anti-β-catenin antibody.

Luciferase Assay—15 ng of the Super 8x TOPFlash luciferase reporter (measures TCF transcriptional activation), or Super 8x FOPFlash as a (control) and 3 ng of phRL-TK vector of *Renilla* luciferase (Promega Biosciences, Madison, WI) as an transfection control were transfected into HEK 293 cells with SuperFect Transfection Reagent (Qiagen, Valencia, CA) following the manufacturer's instructions. 24 h after transfection, cells lysates were used to detect luciferase activity. For each experimental group, the measurements were done in duplicate and repeated at least three times. The data shown are from at least three experiments, and the results are expressed as the mean ±S.D.

GSK3β in Vitro Kinase Assay—2×10^6 cells were lysed, and GSK3β was immunoprecipitated as described above. The beads were washed twice with lysis buffer, twice with wash buffer (500 mM LiCl, 100 mM Tris, pH 7.6, and 0.1% Triton X-100), twice with reaction buffer (20 mM MOPS, pH 7.4, 2 mM EGTA, 10 mM $MgCl_2$, 5 mM MnCl, and 0.1% Triton X-100), then resuspended in the reaction buffer plus [γ-^{32}P]ATP and recombinant β-catenin protein as the substrate. The preparations were incubated at 30 °C for 30 min. For the GSK3β-mediated PDZ-RGS3 phosphorylation, immunoprecipitated PDZ-RGS3 was incubated with recombinant GSK3β (Millipore) in the above reaction buffer at 30 °C for 30 min. The reactions were terminated by the addition of SDS-PAGE sample buffer, and the samples were fractionated by SDS-PAGE to examine substrate phosphorylation and to examine the amount of PDZ-RGS3 in the immunoprecipitations.

Immunofluorescence—MDCK cells seeded on coverglass-bottom microwell dishes were washed once with PBS and fixed in 4% paraformaldehyde in PBS for 20 min at room temperature. These cells were washed with PBS, then treated with 0.2% Triton X-100 in PBS for 10 min to enhance cellular permeability. These cells were stained for the various epithelial and mesenchymal markers for 1 h with specific first antibodies and followed by incubation with the second antibodies labeled with Alexa Fluor 568 for 30 min at room temperature. The dishes were washed 5–6 times in excess PBS and then mounted with Vectashield (Vector Laboratories, Burlingame, CA). The preparations were visualized using a PerkinElmer Life Sciences spinning disk confocal microscope using UltraView software. Live cell imaging of HEK 293 was performed using the same microscope.

RT-PCR—The RNA was isolated with TRIzol® reagent according to the manufacturer's instructions (Invitrogen). The DNAs were synthesized from 1 μg of RNA using an Omniscript RT kit with Omniscript Reverse Transcriptase (Qiagen). Real-time PCR was performed using a 7500 Real-Time PCR System (Invitrogen) following the Rotor-Gene™ SYBR® Green PCR kit (Qiagen) protocol. The following primer sets were used: GAPDH, 5′-CGGAGTCAACGGATTTGGTCG and 5′-GTTCTCAGCCTTGACGGTGC; c-Myc, 5′-CTGGTGCTCCATGAGGAGAC and 5′-GAAGGTGATCCAGACTCTGACC; PDZ-RGS3, 5′-CTACCGCCAGATCACCATCC and 5′-CCACACATTTCCAGTGCTCCAC.

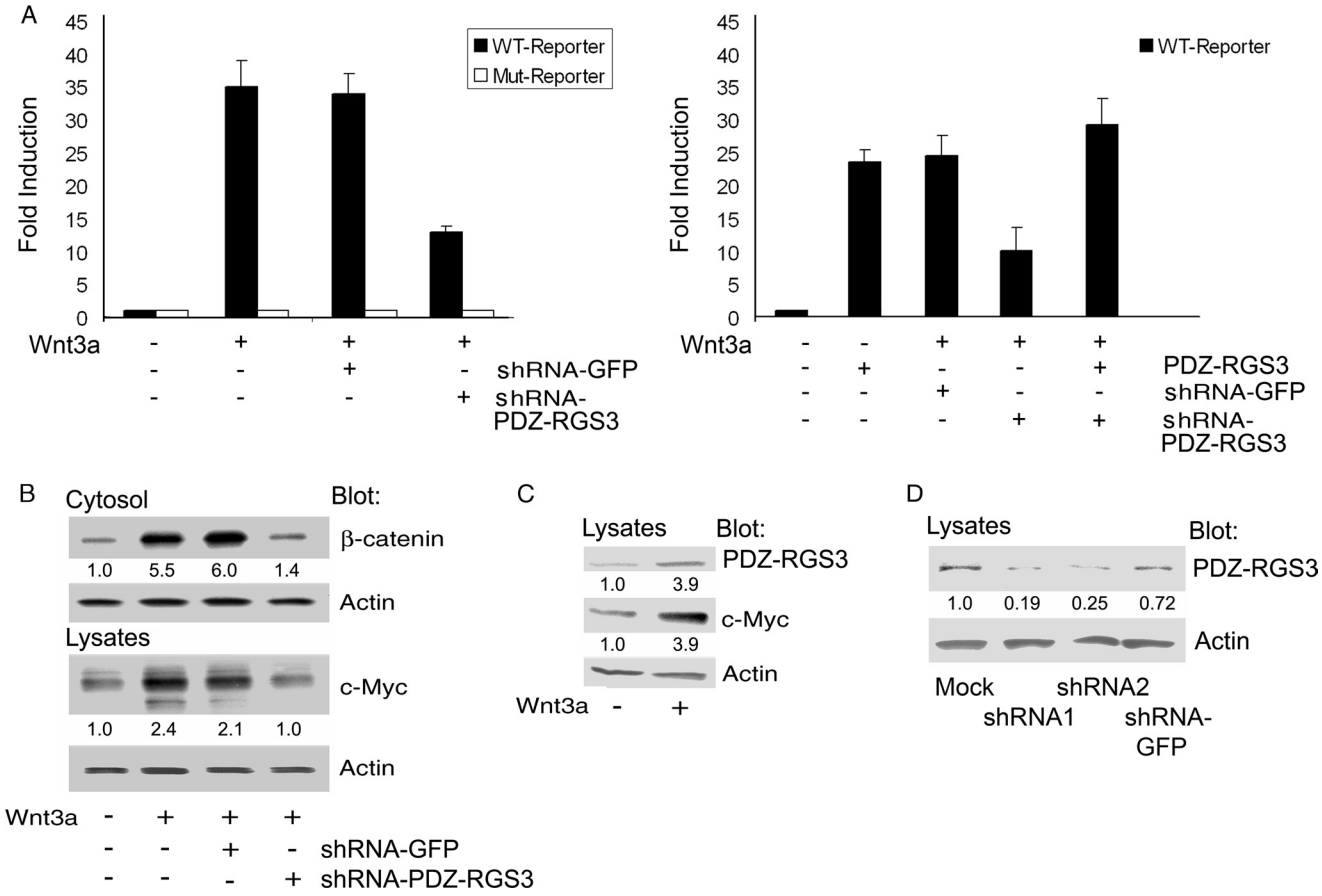

FIGURE 1. **PDZ-RGS3 expression affected Wnt3a-induced activation of the canonical pathway.** *A*, reduced PDZ-RGS3 expression impaired Wnt3a ligand-induced TCF reporter expression. HEK 293 cells were transfected with a TCF luciferase reporter (*WT*, Super 8x TOPFlash luciferase reporter or *Mut*, Super 8x FOPFlash) plus phRL-TK vector. The shRNA2 targeting N-terminal PDZ-RGS3 or the negative shRNA control-targeting GFP plus Wnt3a cDNA were transfected into HEK 293 cells for 24 h. The mouse *Wnt3a* cDNA was used to express the Wnt ligand to drive TCF reporter activation. The -fold induction with mean ±S.D. of three independent experiments is shown. *B*, reduced PDZ-RGS3 expression impaired Wnt3a ligand-mediated cytosolic β-catenin stabilization and enhanced c-Myc expression. The shRNA1-PDZ-RGS3, negative control shRNA-GFP plus *Wnt3a* cDNA constructs were, respectively, transfected into HEK 293 cells for 24 h. The harvested cells were separated into two parts. The first was prepared for cytosolic fraction, and the second was used for total cellular lysates. The cytosolic β-catenin, c-Myc, or actin was immunoblotted. Similar results were obtained in two independent experiments. *C*, Wnt3a treatment increased PDZ-RGS3 levels. HEK 293 cells were transfected with *Wnt3a* cDNA for 24 h. Endogenous PDZ-RGS3, c-Myc, and actin were, respectively, blotted with their antibodies. Similar results were obtained in two independent experiments. *D*, PDZ-RGS3 shRNAs reduce endogenous PDZ-RGS3 expression. HEK 293 cells were transfected with two shRNAs (indicated *shRNA1* and *shRNA2*) targeting the different sites of N-terminal PDZ-RGS3, and a negative control shRNA targeting GFP for 48 h. The blots of PDZ-RGS3 and a loading control actin are shown.

RESULTS

PDZ-RGS3 Expression Affects β-Catenin Stability and Signaling—We initially thought that reducing PDZ-RGS3 expression would enhance Wnt3a signaling by increasing the duration that any activated $G\alpha_{o/i}$ remained GTP-bound. To test that hypothesis, we transfected HEK 293 cells with a Wnt3a expression vector along with a TCF luciferase reporter construct or a suitable control in the presence of a control or PDZ-RGS3-specific shRNA. The production of Wnt3a will result in the activation of the co-transfected TCF reporter. Surprisingly, the depletion of PDZ-RGS3 gave us the opposite result from what we had anticipated as it impaired Wnt3a-induced TCF reporter activity ~60% (Fig. 1*A*, *left panel*).

Based on this result, we checked whether increased levels of PDZ-RGS3 affected TCF reporter activity. We found that transfection of the PDZ-RGS3 construct in the absence of the Wnt3a expression vector resulted in a potent induction of the TCF reporter. Furthermore, PDZ-RGS3 expression readily overcame the TCF reporter activity impairment produced by the PDZ-RGS3 knock-down in Wnt3a-expressing cells (Fig. 1*A*, *right panel*).

To verify the PDZ-RGS3 knock-down result, we examined the accumulation of cytosolic β-catenin and c-*myc* expression, a known Wnt target gene (19), following Wnt3a stimulation. In accordance with the TCF reporter assay results, we found that the reduction of PDZ-RGS3 blunted the accumulation of cytosolic β-catenin and reduced the increase in c-*myc* triggered by Wnt3a signaling (Fig. 1*B*).

Wnt signaling is known to induce proteins that impact subsequent signaling. For example, it increases Axin2 expression, which negatively regulates the signaling pathway (20–22). To test whether Wnt signaling affected PDZ-RGS3 expression, we transfected the Wnt3a construct into HEK 293 cells and immunoblotted the cell lysates for endogenous PDZ-RGS3 and c-Myc as a positive control. We found a nearly 4-fold increase in both proteins (Fig. 1*C*). The reduction of PDZ-RGS3 by the two shRNAs is shown (Fig. 1*D*). Together these results indicate

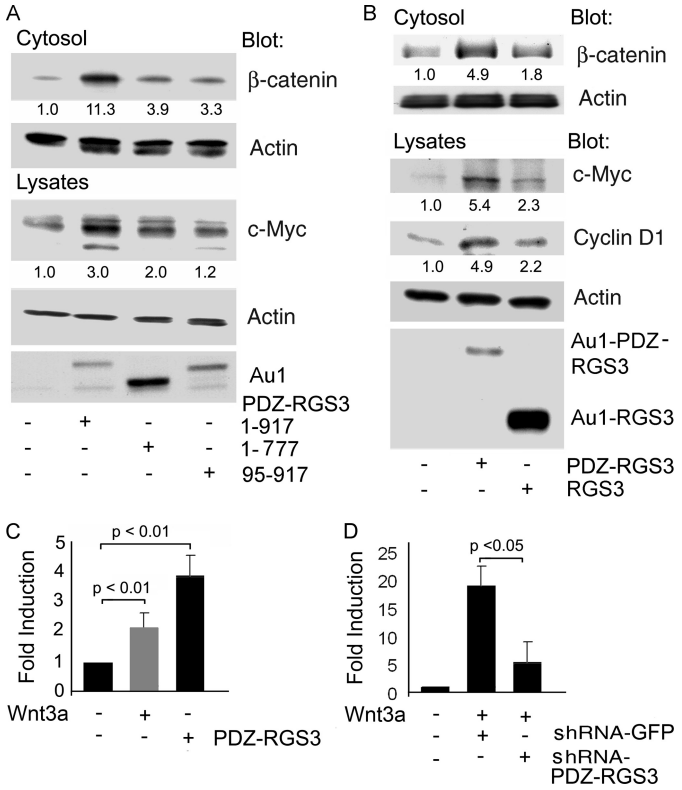

FIGURE 2. **PDZ-RGS3, but not RGS3, enhanced canonical Wnt signaling.** *A*, PDZ and RGS domains of PDZ-RGS3 were needed to increase cytosolic β-catenin levels and facilitate expression of c-Myc. HEK 293 cells were transfected with full-length PDZ-RGS3, RGS-deleted (1–777) or PDZ-deleted (95–917) domain truncated constructs for 24 h. The cells were separated, one half for the cytosolic fraction and the other half for total cell lysates. The levels of cytosolic β-catenin, c-Myc, PDZ-RGS3, and actin were immunoblotted. *B*, PDZ-RGS3, but not RGS3, induced expressions of c-Myc and cyclin D1. PDZ-RGS3 or RGS3 was transfected into HEK 293 cells. The indicated proteins from the total cell lysates were detected by immunoblotting. Similar results were obtained in three independent experiments. *C*, Wnt3a stimulation increased PDZ-RGS3 expression, and PDZ-RGS3 increased c-Myc. RNA extracted from either Wnt3a- or PDZ-RGS3-transfected HEK 293 cells was analyzed by quantitative PCR for PDZ-RGS3 (*gray*) or c-Myc (*black*). Results are -fold increase compared with nonstimulated controls following normalization to GAPDH expression and from three separate experiments. *D*, Wnt3a-stimulated increase in c-Myc expression was inhibited by a PDZ-RGS3 shRNA. RNA extracted from Wnt3a and either control or PDZ-RGS3 shRNA-transfected HEK 293 cells was analyzed by quantitative PCR for c-Myc. Results are -fold increase compared with nonstimulated controls following normalization to GAPDH expression and from three separate experiments.

that the levels of PDZ-RGS3 affect Wnt-mediated activation of the canonical pathway.

Both the RGS and PDZ Domains of PDZ-RGS3 Are Needed for β-Catenin Stabilization—We transfected constructs expressing either full-length PDZ-RGS3, an RGS domain-deleted form or a PDZ domain-deleted version. A schematic of the constructs is shown in supplemental Fig. S1. The levels of cytosolic actin served as a loading control. Whereas full-length PDZ-RGS3 increased the levels of cytosolic β-catenin and c-*myc*, the RGS domain or PDZ domain-deleted versions had much less effect (Fig. 2*A*). We also compared PDZ-RGS3 with RGS3L, which contains the C-terminal 519 amino acids of PDZ-RGS3 (16). Expression of PDZ-RGS3 increased cyclin D1, another Wnt target gene (23), and c-*myc* whereas RGS3L expression had only a modest effect despite its much higher expression (Fig. 2*B*). Next, we verified that the induction of PDZ-RGS3 by Wnt3a and c-*myc* expression by PDZ-RGS3 occurred at the transcription level by performing quantitative RT-PCR using the appropriately stimulated cells (Fig. 2*C*). We also corroborated the reduction in Wnt3a-induced TCF reporter gene activity by the PDZ-RGS3 shRNA showing that it also reduced Wnt3a-induced elevation of c-*myc* mRNAs (Fig. 2*D*). These data provided additional evidence for the modulation of Wnt signaling by PDZ-RGS3 and implicated the PDZ and RGS domains as being functionally importance.

PDZ-RGS3 Impairs GSK3β-mediated Phosphorylation of β-Catenin in Vitro and May Serve as a GSK3β Substrate—To check whether PDZ-RGS3 altered GSK3β kinase activity, we performed an *in vitro* kinase assay using recombinant β-catenin protein as a substrate. The expression of PDZ-RGS3 inhibited β-catenin phosphorylation. We also found that Wnt3a reduced β-catenin phosphorylation in the assay (Fig. 3*A*). Next, we immunoblotted cell lysates prepared from HEK 293 cells expressing PDZ-RGS3, RGS3, or Wnt3a using antibodies directed against phosphorylated β-catenin. PDZ-RGS3 and to a less extent RGS3 expression reduced the amount of Ser-33/Ser-37/Thr-41-phosphorylated β-catenin. We also examined whether GSK3β could phosphorylate PDZ-RGS3. GSK3β was incubated with immunoprecipitated PDZ-RGS. Suggesting that this is the case, a band of the appropriate size for PDZ-RGS3 was phosphorylated (Fig. 3*B*). These results indicated that a PDZ-RGS3/GSK3β interaction might contribute to the regulation of β-catenin stability.

Wnt Signaling Enhances the PDZ-RGS3/GSK3β Interaction—We expressed PDZ-RGS3 in HEK 293 cells and treated the cells with recombinant Wnt3a for 15 min. GSK3β immunoprecipitates contained tagged PDZ-RGS3, but Wnt signaling did not alter the amount of protein in the complex. We also noted that whereas Gsk3β immunoprecipitates contained Dvl, PDZ-RGS3 immunoprecipitates did not (Fig. 4*A*). The failure to observe an effect of Wnt signaling on the GSK3β/PDZ-RGS3 interaction using transfected PDZ-RGS3 led us to test whether endogenous PDZ-RGS3 might behave differently. Indeed, we found that Wnt signaling enhanced the amount of endogenous PDZ-RGS3 in the GSK3β immunoprecipitates (Fig. 4*B*).

GSK3β Interacts with PDZ-RGS3 or Axin1—The phosphorylation of β-catenin is facilitated by the interactions of Axin1, adenomatous polyposis coli, and GSK3 (24, 25). To better understand how PDZ-RGS3 and Axin1 function to affect β-catenin stability, we examined whether these proteins could both bind GSK3β. We transfected Au1-tagged PDZ-RGS3 and Myc-tagged Axin1 into HEK 293 cells. The GSK3β immunoprecipitates contained both PDZ-RGS3 and Axin1; however, Axin1 immunoprecipitates lacked PDZ-RGS3 and vice versa (Fig. 5*A*). Next, we examined the relative preference of GSK3β for Axin1 *versus* PDZ-RGS3. Increased Axin1 expression reduced the GSK3β-PDZ-RGS3 interaction whereas increased PDZ-RGS3 expression did not impact the Axin1-GSK3β interaction (Fig. 5, *B* and *C*). To test whether increased Axin1 expression affected the PDZ-RGS3-induced cytosolic β-catenin accumulation, we co-expressed both proteins and examined cytosolic β-catenin levels. Axin1 overexpression completely reversed the increase in cytosolic β-catenin we had observed following the overexpression of PDZ-RGS3 (Fig. 5*D*).

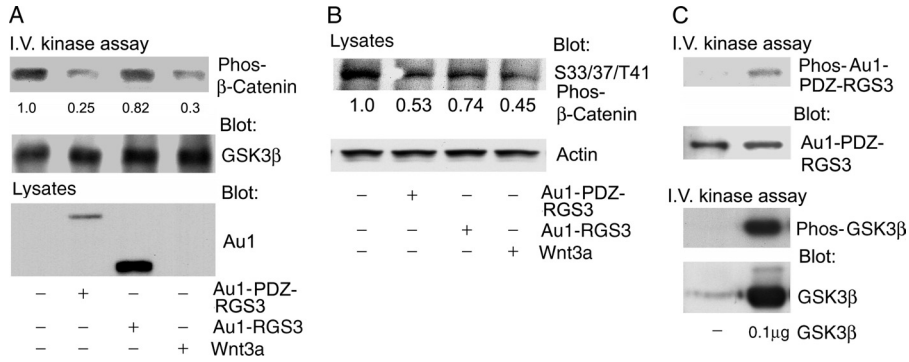

FIGURE 3. **PDZ-RGS3 impaired β-catenin phosphorylation by GSK3β and served as GSK3β substrate.** *A*, *in vitro* kinase assay was used to examine GSK3β kinase activity. PDZ-RGS3, RGS3, or Wnt3a was expressed in HEK 293 cells. Endogenous GSK3β was immunoprecipitated, and recombinant β-catenin was used as the substrate. The phosphorylated β-catenin (*first panel*) and immunoprecipitated GSK3β (*second panel*) are shown. The *bottom panel s*hows the levels of PDZ-RGS3 and RGS3 in the cell lysate. *B*, immunoblot of lysates prepared from HEK293 cells was transfected with the indicated plasmids and treated with MG132 (10 μM) for the last 4 h to examine the level of phosphorylated β-catenin. Actin was used as a loading control. *C*, PDZ-RGS3 was phosphorylated by GSK3β. Immunoprecipitated Au1-tagged PDZ-RGS3 was incubated with a recombinant GSK3β. Phosphorylated PDZ-RGS3, immunoprecipitated PDZ-RGS3, phosphorylated GSK3β, and GSK3β levels are shown. Similar results were obtained in two independent experiments.

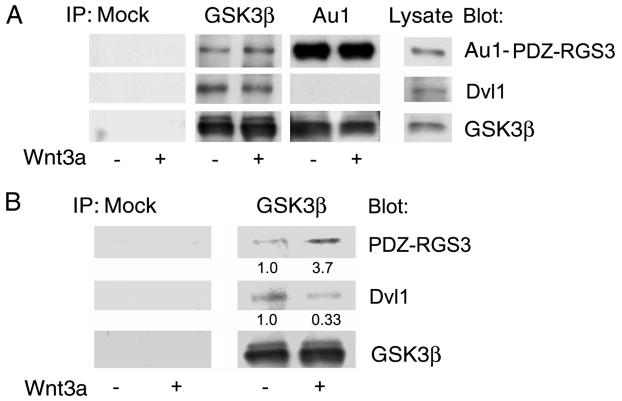

FIGURE 4. **PDZ-RGS3 interacted with GSK3β but not Dvl.** *A*, PDZ-RGS3 was co-immunoprecipitated with GSK3β. HEK 293 cells transiently transfected with Au1-tagged PDZ-RGS3 were treated with Wnt3a (20 ng/ml) or not for 15 min. The lysates were used for immunoprecipitation and immunoblots with the indicated antibodies. *B*, Wnt3a increased the endogenous GSK3β and PDZ-RGS3 interaction, but reduced the GSK3β and Dvl1 interaction. HEK 293 cells were treated with Wnt3a ligand (20 ng/ml) for 15 min. The cells were lysed and GSK3β immunoprecipitated. The indicated proteins were detected by immunoblotting.

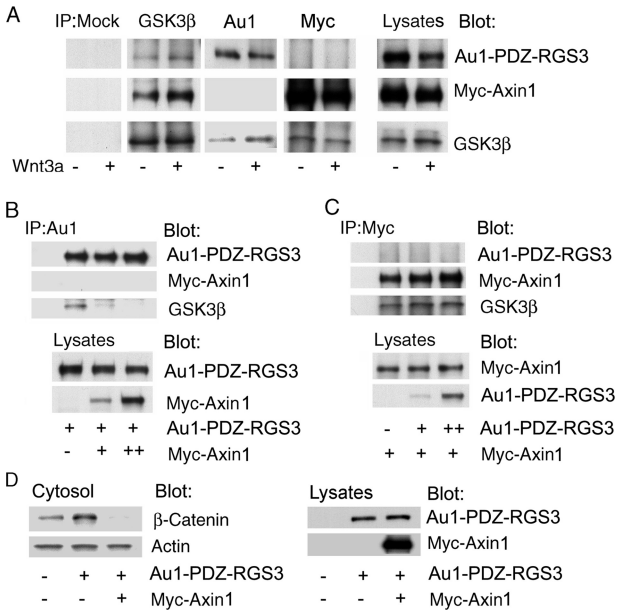

FIGURE 5. **Axin1 preferentially interacted with GSK3β as compared with PDZ-RGS3.** *A*, interaction of PDZ-RGS3 or Axin1 with endogenous GSK3β. Au1-PDZ-RGS3 or Myc-Axin1 was transfected into HEK 293 cells along with *Wnt3a* cDNA or not. Endogenous GSK3β was immunoprecipitated, and the amount of co-immunoprecipitating PDZ-RGS3 or Axin1 is shown. The *last column* shows the indicated proteins in the cell lysates. *B*, increased Axin1 expression impaired the PDZ-RGS3 and GSK3β interaction. HEK 293 cells were transfected with Au1-PDZ-RGS3 and increasing amounts of Myc-Axin1. The cellular lysates were immunoprecipitated with nonspecific antibodies (*lane 1*) or Au1 antibodies (*lanes 2–4*). Immunoblotting was used to detect the indicated proteins. *C*, increased PDZ-RGS3 expression did not affect the Axin1 and endogenous GSK3β interaction. HEK 293 cells were transfected with Myc-Axin1 and increasing amounts of Au1-PDZ-RGS3. The cellular lysates were immunoprecipitated with nonspecific antibodies (*lane 1*) or anti-Myc. The indicated proteins were determined by immunoblotting. *D*, Axin1 impaired the effect of PDZ-RGS3 on cytosolic β-catenin. HEK 293 cells expressing PDZ-RGS3 in the presence or absence of Axin1 were immunoblotted for cytosolic β-catenin and cytosolic actin. The *right panels* show PDZ-RGS3 and Axin1 expression in the cell lysates. Similar results were obtained in three independent experiments.

These results suggest that PDZ-RGS3 targets a pool of GSK3β not associated with destruction complex.

*PDZ-RGS3 Expression Triggers EMT—S*nail1 is a transcriptional repressor that controls E-cadherin and regulates EMT. Snail1 is a GSK3β target being phosphorylated on two distinct motifs, the first one directs Snail1 ubiquitination and proteolytic destruction whereas the second site regulates nuclear export and repressor function (6, 7). To determine whether PDZ-RGS3 could impact Snail1 stability, we first examined whether depleting PDZ-RGS3 Wnt3a induced an increase in Snail1 expression and a decrease in E-cadherin. When we lowered PDZ-RGS3 expression using shRNAs, the Wnt3A-mediated changes in Snail1 and E-cadherin protein levels were reduced as compared with Wnt3a-treated cells expressing a control shRNA (Fig. 6*A*). Conversely, overexpressing of PDZ-RGS3 enhanced Snail1 and reduced E-cadherin expression whereas RGS3 had much less effect (Fig. 6*B*). These results suggested that PDZ-RGS3 might affect Wnt signaling-induced EMT. To test that possibility, we generated MDCK cell lines stably transfected with PDZ-RGS3-GFP, RGS3-GFP, or GFP vector. MDCK cells are known to undergo EMT following exposure to Wnt3a. Live cell imaging revealed that the cells, which expressed PDZ-RGS3-GFP, lost their typical epithelial cell characteristics and acquired a spindle appearance; whereas, the morphology of the RGS3-GFP-expressing cell line resem-

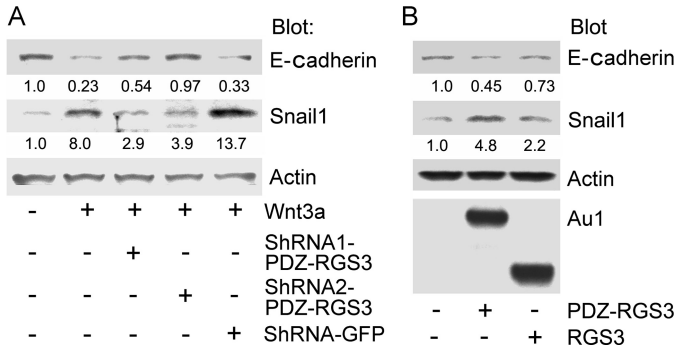

FIGURE 6. **PDZ-RGS3 expression levels modulated Wnt3a signaling.** *A*, reduced PDZ-RGS3 expression impaired Wnt3a-induced stabilization of Snail1 and reduction of E-cadherin. Cell lysates from HEK 293 cells expressing Wnt3a along with the indicated shRNAs were immunoblotted for the indicated proteins. *B*, overexpression of PDZ-RGS3, but not RGS3, enhanced Snail1 (*Snail*) and reduced E-cadherin expression. HEK 293 cells or HEK 293 cells expressing PDZ-RGS3 or RGS3 were immunoblotted with antibodies against the indicated proteins.

bled the GFP-expressing MDCK cells. Stimulation of GFP vector-expressing cells with recombinant Wnt3a led to a morphology similar to that observed with the PDZ-RGS3-expressing cells in the absence of Wnt3a (Fig. 7*A*). To confirm that the morphology changes were because of EMT, we immunostained the different cell lines for the expression of E-cadherin and fibronectin. As a consequence of EMT, E-cadherin levels decline whereas fibronectin increase. Stimulation of the GFP vector cells with Wnt3a as expected decreased E-cadherin and increased fibronectin. These cells resembled the PDZ-RGS3-GFP-expressing cells whereas the RGS3-GFP-expressing cells resembled the untreated GFP vector cells (Fig. 7, *B* and *C*). These results show that high levels of PDZ-RGS3 can promote EMT by affecting the β-catenin stability.

Finally, we transiently transfected constructs expressing either PDZ-RGS3 GFP, PDZ-RGS3 shRNA GFP, or a control shRNA GFP into HEK 293 cells and examined the resulting morphology of the GFP-positive cells. Live cell imaging revealed that PDZ-RGS3 induced a spindle-like cell morphology similar to what we had observed with the MDCK cells. In contrast, the cells expressing the PDZ-RGS3 shRNA were rounder and smaller than the cells expressing the control shRNA. These results indicate that PDZ-RGS3 expression levels may impact the morphology of a variety of cell types (supplemental Fig. S2).

DISCUSSION

In this article we demonstrated that PDZ-RGS3 affects signaling through the canonical Wnt pathway. We found that lowering the PDZ-RGS3 levels reduced Wnt3a signaling whereas raising PDZ-RGS3 levels mimicked activation of the canonical Wnt pathway. PDZ-RGS3 co-immunoprecipitated with GSK3β, and its expression reduced GSK3β kinase activity toward β-catenin. The GSK3β-binding sites for Axin1 and PDZ-RGS3 may overlap as Axin1 and PDZ-RGS3 immunoprecipitates did not contain the reciprocal protein although both contained GSK3β. The introduction of PDZ-RGS3 into MDCK cells resulted in a phenotype consistent with cells that have undergone an epithelial to mesenchymal transition.

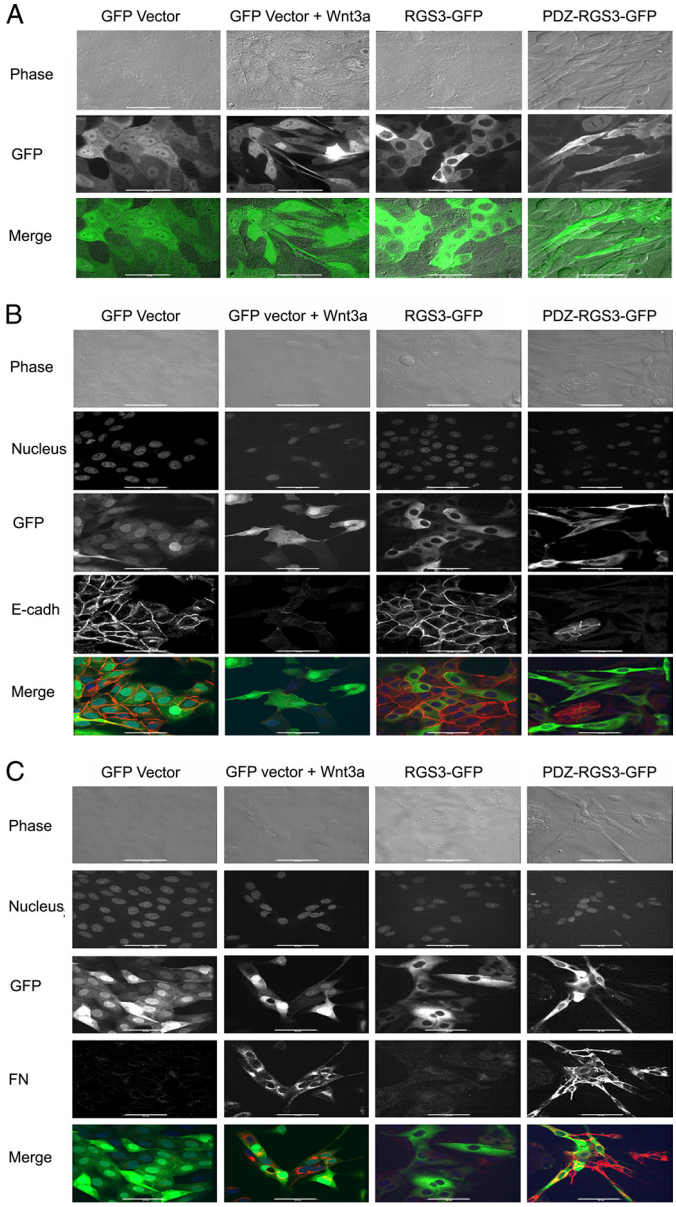

FIGURE 7. **PDZ-RGS3 expression mimicked Wnt3a treatment of MDCK cells and triggers EMT.** *A*, Wnt3a treatment or PDZ-RGS3 expression, but not RGS3 expression, caused MDCK cells to lose their epithelial characteristics. Stable MDCK transfectants of GFP vector, RGS3-GFP, or PDZ-RGS3-GFP were generated. Images of live cells are shown. The indicated cells were exposed to Wnt3a (20 ng/ml) overnight. *B*, Wnt3a and PDZ-RGS3 expression decreased E-cadherin expression. The indicated cells were immunostained for E-cadherin (*red*). *Phase contrast*, nucleus (far red), green fluorescent, and red fluorescent images were acquired. An E-cadherin (*red*) with GFP (*green*) merge is also shown. *C*, Wnt3a treatment or PDZ-RGS3 expression increased fibronectin (*FN*) expression. The cells stably transfected with indicated constructs were fixed and immunostained for fibronectin. *Phase contrast*, nucleus (*far red*), GFP (*green*), and fibronectin (*red*) images were acquired. A merged image between GFP and fibronectin is shown in the *bottom panels*. *Scale bar*, 20 μm.

Upon Wnt binding, Frizzled receptors activate the heterotrimeric G-protein Gα_o, which helps to recruit the destruction complex to the plasma membrane (26). Gα_o-released G$\beta\gamma$ subunits bind and assist the relocalization of Dvl to the plasma membrane, where Dvl binds the receptor via its PDZ domain and oligomerizes along with LRP5/6. This provides a platform for the destruction complex relocation (27). Based on this

model, the reduction of PDZ-RGS3 should have enhanced Wnt signaling by reducing the duration that G_o remains GTP bound and $G\beta\gamma$ available to recruit Dvl to membrane. However, revealing a different functional role, lowering PDZ-RGS3 levels inhibited Wnt-induced activation of the canonical pathway.

According to a recent report, Wnt signaling inhibits β-catenin degradation by suppressing β-catenin ubiquitination (4). This occurs without obvious destruction complex disassembly or reduced Axin1-bound β-catenin phosphorylation. Rather Wnt signaling causes the dissociation of the ubiquitin ligase βTrCP from the destruction complex. This blocks proteasomal removal of β-catenin jamming the destruction complex (4). How PDZ-RGS3 fits into this scenario is not clear. We have no evidence that PDZ-RGS3 is present in the destruction complex as it did not immunoprecipitate with Axin1, the central scaffolding protein and rate-limiting factor in complex formation. It also did not co-immunoprecipitate with Dvl. Without a direct link to the destruction complex, it is difficult to invoke a role for PDZ-RGS3 in complex recruitment or βTrCP release. Perhaps PDZ-RGS3 negatively regulates a second GSK3β-containing complex that also governs β-catenin stability. Wnt signaling raised PDZ-RGS3 expression. Interfering with this induction would impair the negative feedback and reduce Wnt-triggered increases in cytosolic β-catenin as we observed. To account for the PDZ-RGS3 overexpression phenotype, inhibition of the same complex would increase β-catenin stability. This might occur despite the continued activity of the Axin1 destruction complex because of the relative scarcity of Axin1 *versus* PDZ-RGS3 and GSK3β.

PDZ-RGS3 shares some feature with frequently rearranged in advanced T cell (FRAT), another GSK3β-binding protein (29, 30). FRAT proteins reduce GSK3β kinase activity, and like PDZ-RGS3, FRAT protein expression leads to a potent activation of canonical Wnt signal transduction However, FRAT interacts with Axin1 and with several other proteins involved in regulating Wnt signaling whereas PDZ-RGS3 did not. Surprisingly *FRAT1/FRAT2/FRAT3* triple knock-out mice proved viable without an overt phenotype, raising a question about the role of FRAT proteins in Wnt signaling (31). Nevertheless, assessing whether FRAT proteins and PDZ-RGS3 collaborate to regulate GSK3β seems warranted.

Both the PDZ and RGS domains in PDZ-RGS3 were needed for the stabilization of β-catenin. In addition, RGS3, which has the same RGS domain as PDZ-RGS3, had much less effect on β-catenin stability, and it did not stimulate EMT in MDCK cells. Whether the GAP activity of PDZ-RGS3 is needed for β-catenin stabilization is unresolved, although it seems unlikely. Further experiments with point mutants and chimeric constructs will help resolve the importance of the different domains in PDZ-RGS3 for β-catenin stabilization.

Whereas our focus has been the role of PDZ-RGS3 in the regulation of canonical Wnt signaling, two reports using zebrafish as a model organism have implicated RGS proteins in the regulation of noncanonical Wnt signaling (32, 33). RGS3 function was shown to be necessary for the appropriate frequency and amplitude of calcium release during somitogenesis and RGS18 for the development of cilia in hair cells of the inner ear and neuromast cells and for normal platelet numbers. Remarkably, depletion of Wnt5b led to the same spectrum of phenotypes as were observed following interference with RGS18 or RGS3 (32, 33). In the RGS3 interference study, the phenotype could be rescued by a short RGS3 isoform (165 amino acids), but not by a RGS3 protein $rgs3^{N109A}$, which lacks GAP activity (33). The zebrafish RGS3 protein is highly homologous to the C-terminal portions of human RGS3L and PDZ-RGS3 used in this study. Thus, RGS3 and its various isoforms may serve several roles in Wnt signaling impacting both the canonical and noncanonical pathways.

PDZ-RGS3 via its PDZ domain can interact with the three known Ephrin-B types to link Ephrin-B signaling to the regulation of Gα proteins (17). Specifically targeting the expression of PDZ-RGS3 in mice by introducing LoxP sites flanking exons 2–5 allowed deletion of the PDZ domain without affecting the expression of RGS3 isoforms generated from downstream exons. The disruption of the coding region for the PDZ domain of RGS3 in mice resulted in smaller mice and caused an early cell cycle exit and precocious differentiation of neural progenitors in the cerebral cortex (18). The mutation also decreased early mouse viability. At 3 weeks of age, fewer than expected homozygous mutant mice were recovered. Whereas the phenotype was explained on the basis of loss of the Ephrin-B/RGS pathway, our study indicates that the loss of PDZ-RGS3 may have impacted Wnt signaling as well.

Snail factors are transcriptional repressors downstream of Wnt/β-catenin signaling, which have been linked to the formation of cancer stem cells, and their increased expression can trigger EMT (6–8). We found that the knockdown of PDZ-RGS3 impaired Wnt3a-induced Snail1 expression and that PDZ-RGS3 expression in HEK 293 cells increased Snail1 expression. Consistent with that observation, overexpression of PDZ-RGS3 in MDCK cells led to morphological changes consistent with EMT. In contrast, RGS3 overexpression did not cause such changes. These data support a further examination of PDZ-RGS3 in cancer stem cell biology. RGS3 has been shown to be up-regulated in p53-mutated breast cancer samples and associated with a resistance to the chemotherapeutic agent docetaxel (34). In that study, the reagents employed would not have distinguished among the various RGS isoforms so their relative importance is unknown. In conclusion, our data and others have implicated RGS3 isoforms in the regulation of Wnt signaling and EMT and provide a basis of further study of RGS3 and its various isoforms.

Acknowledgments—We thank Mary Rust for excellent editorial assistance; Dr. Anthony Fauci for continued support, and Dr. Randall Moon for providing us the Super 8x TOPFlash and Super 8x FOPFlash luciferase reporter constructs.

REFERENCES

1. Huelsken, J., and Behrens, J. (2002) The Wnt signaling pathway. *J. Cell Sci.* **115,** 3977–3988
2. Miller, J. R., Hocking, A. M., Brown, J. D., and Moon, R. T. (1999) Mechanism and function of signal transduction by the Wnt/β-catenin and Wnt/Ca^{2+} pathways. *Oncogene* **18,** 7860–7872
3. Veeman, M. T., Axelrod, J. D., and Moon, R. T. (2003) A second canon: functions and mechanisms of β-catenin-independent Wnt signaling. *Dev.*

Cell **5,** 367–377
4. Li, V. S., Ng, S. S., Boersema, P. J., Low, T. Y., Karthaus, W. R., Gerlach, J. P., Mohammed, S., Heck, A. J., Maurice, M. M., Mahmoudi, T., and Clevers, H. (2012) Wnt signaling through inhibition of β-catenin degradation in an intact axin1 complex. *Cell* **149,** 1245–1256
5. Gordon, M. D., and Nusse, R. (2006) Wnt signaling: multiple pathways, multiple receptors, and multiple transcription factors. *J. Biol. Chem.* **281,** 22429–22433
6. Zhou, B. P., Deng, J., Xia, W., Xu, J., Li, Y. M., Gunduz, M., and Hung, M. C. (2004) Dual regulation of snail by GSK3β-mediated phosphorylation in control of epithelial-mesenchymal transition. *Nat. Cell Biol.* **6,** 931–940
7. Yook, J. I., Li, X. Y., Ota, I., Fearon, E. R., and Weiss, S. J. (2005) Wnt-dependent regulation of the E-cadherin repressor snail. *J. Biol. Chem.* **280,** 11740–11748
8. Yook, J. I., Li, X. Y., Ota, I., Hu, C., Kim, H. S., Kim, N. H., Cha, S. Y., Ryu, J. K., Choi, Y. J., Kim, J., Fearon, E. R., and Weiss, S. J. (2006) A Wnt-axin2-GSK3β cascade regulates snail1 activity in breast cancer cells. *Nat. Cell Biol.* **8,** 1398–1406
9. Lee, J. M., Dedhar, S., Kalluri, R., and Thompson, E. W. (2006) The epithelial-mesenchymal transition: new insights in signaling, development, and disease. *J. Cell Biol.* **172,** 973–981
10. Zhou, B. P., and Hung, M. C. (2005) Wnt, hedgehog and snail: sister pathways that control by GSK3β and βTrCP in the regulation of metastasis. *Cell Cycle* **4,** 772–776
11. Scheel, C., and Weinberg, R. A. (2011) Phenotypic plasticity and epithelial-mesenchymal transitions in cancer and normal stem cells? *Int. J. Cancer* **129,** 2310–2314
12. Castellone, M. D., Teramoto, H., Williams, B. O., Druey, K. M., and Gutkind, J. S. (2005) Prostaglandin E_2 promotes colon cancer cell growth through a G_s-axin-β-catenin signaling axis. *Science* **310,** 1504–1510
13. Stemmle, L. N., Fields, T. A., and Casey, P. (2006) The regulator of G-protein signaling domain of axin selectively interacts with $G\alpha_{12}$ but not $G\alpha_{13}$. *Mol. Pharmacol.* **70,** 1461–1468
14. Kehrl, J. H. (1998) Heterotrimeric G-protein signaling: roles in immune function and fine-tuning by RGS proteins. *Immunity* **8,** 1–10
15. Cho, H., and Kehrl, J. H. (2009) Regulation of immune function by G-protein-coupled receptors, trimeric G-proteins, and RGS proteins. *Prog. Mol. Biol. Transl. Sci.* **86,** 249–298
16. Kehrl, J. H., Srikumar, D., Harrison, K., Wilson, G. L., and Shi, C. S. (2002) Additional 5′ exons in the RGS3 locus generate multiple mRNA transcripts, one of which accounts for the origin of human PDZ-RGS3. *Genomics* **79,** 860–868
17. Lu, Q., Sun, E. E., Klein, R. S., and Flanagan, J. G. (2001) Ephrin-B reverse signaling is mediated by a novel PDZ-RGS protein and selectively inhibits G-protein-coupled chemoattraction. *Cell* **105,** 69–79
18. Qiu, R., Wang, J., Tsark, W., and Lu, Q. (2010) Essential role of PDZ-RGS3 in the maintenance of neural progenitor cells. *Stem Cells* **28,** 1602–1610
19. He, T. C., Sparks, A. B., Rago, C., Hermeking, H., Zawel, L., da Costa, L. T., Morin, P. J., Vogelstein, B., and Kinzler, K. W. (1998) Identification of c-Myc as a target of the APC pathway. *Science* **281,** 1509–1512
20. Yan, D., Wiesmann, M., Rohan, M., Chan, V., Jefferson, A. B., Guo, L., Sakamoto, D., Caothien, R. H., Fuller, J. H., Reinhard, C., Garcia, P. D., Randazzo, F. M., Escobedo, J., Fantl, W. J., and Williams, L. T. (2001) Elevated expression of axin2 and hnkd mRNA provides evidence that Wnt/β-catenin signaling is activated in human colon tumors. *Proc. Natl. Acad. Sci. U.S.A.* **98,** 14973–14978
21. Lustig, B., Jerchow, B., Sachs, M., Weiler, S., Pietsch, T., Karsten, U., van de Wetering, M., Clevers, H., Schlag, P. M., Birchmeier, W., and Behrens, J. (2002) Negative feedback loop of Wnt signaling through upregulation of conductin/axin2 in colorectal and liver tumors. *Mol. Cell. Biol.* **22,** 1184–1193
22. Jho, E. H., Zhang, T., Domon, C., Joo, C. K., Freund, J. N., and Costantini, F. (2002) Wnt/β-catenin/TCF signaling induces the transcription of *axin2*, a negative regulator of the signaling pathway. *Mol. Cell Biol.* **22,** 1172–1183
23. Tetsu, O., and McCormick, F. (1999) β-Catenin regulates expression of cyclin D_1 in colon carcinoma cells. *Nature* **398,** 422–426
24. Ikeda, S., Kishida, S., Yamamoto, H., Murai, H., Koyama, S., and Kikuchi, A. (1998) Axin, a negative regulator of the Wnt signaling pathway, forms a complex with GSK3β and β-catenin and promotes GSK3β-dependent phosphorylation of β-catenin. *EMBO J.* **17,** 1371–1384
25. Sakanaka, C., Weiss, J. B., and Williams, L. T. (1998) Bridging of β-catenin and glycogen synthase kinase 3β by axin and inhibition of β-catenin-mediated transcription. *Proc. Natl. Acad. Sci. U.S.A.* **95,** 3020–3023
26. Egger-Adam, D., and Katanaev, V. L. (2010) The trimeric G-protein G_o inflicts a double impact on axin in the Wnt/Frizzled signaling pathway. *Dev. Dyn.* **239,** 168–183
27. Koval, A., Purvanov, V., Egger-Adam, D., and Katanaev, V. L. (2011) Yellow submarine of the Wnt/Frizzled signaling: submerging from the G-protein harbor to the targets. *Biochem. Pharmacol.* **82,** 1311–1319
28. Deleted in proof
29. Deleted in proof
30. Deleted in proof
31. van Amerongen, R., Nawijn, M., Franca-Koh, J., Zevenhoven, J., van der Gulden, H., Jonkers, J., and Berns, A. (2005) FRAT is dispensable for canonical Wnt signaling in mammals. *Genes Dev.* **19,** 425–430
32. Freisinger, C. M., Fisher, R. A., and Slusarski, D. C. (2010) Regulator of G-protein signaling 3 modulates Wnt5b calcium dynamics and somite patterning. *PLoS Genet.* (2010) **6,** e1001020
33. Louwette, S., Labarque, V., Wittevrongel, C., Thys, C., Metz, J., Gijsbers, R., Debyser, Z., Arnout, J., Van Geet, C., and Freson. K. (2012) Regulator of G-protein signaling 18 controls megakaryopoiesis and the cilia-mediated vertebrate mechanosensory system. *FASEB J.* **5,** 2121–2136
34. Ooe, A., Kato, K., and Noguchi, S. (2007) Possible involvement of CCT5, RGS3, and YKT6 genes up-regulated in p53-mutated tumors in resistance to docetaxel in human breast cancers. *Breast Cancer Res. Treat.* **101,** 305–315